RESEARCH REPORTS
Biomaterials & Bioengineering

R. Osorio[1]*, E. Osorio[1], A.L. Medina-Castillo[2], and M. Toledano[1]

[1]Dental School, University of Granada, Colegio Maximo, Campus de Cartuja s/n, 18017 Granada, Spain; and [2]NanoMyP, Spin-Off Enterprise from University of Granada, Edificio BIC-Granada, Av. Innovación 1, 18016 Armilla, Granada, Spain; *corresponding author, rosorio@ugr.es

J Dent Res 93(12):1258-1263, 2014

Polymer Nanocarriers for Dentin Adhesion

ABSTRACT

To obtain more durable adhesion to dentin, and to protect collagen fibrils of the dentin matrix from degradation, calcium- and phosphate-releasing particles have been incorporated into the dental adhesive procedure. The aim of the present study was to incorporate zinc-loaded polymeric nanocarriers into a dental adhesive system to facilitate inhibition of matrix metalloproteinases (MMPs)-mediated collagen degradation and to provide calcium ions for mineral deposition within the resin-dentin bonded interface. PolymP-***n***Active nanoparticles (nanoMyP) were zinc-loaded through 30-minute $ZnCl_2$ immersion and tested for bioactivity by means of 7 days' immersion in simulated body fluid solution (the Kokubo test). Zinc-loading and calcium phosphate depositions were examined by scanning and transmission electron microscopy, elemental analysis, and x-ray diffraction. Nanoparticles in ethanol solution infiltrated into phosphoric-acid-etched human dentin and Single Bond (3M/ESPE) were applied to determine whether the nanoparticles interfered with bonding. Debonded sticks were analyzed by scanning electron microscopy. A metalloproteinase collagen degradation assay was also performed in resin-infiltrated dentin with and without nanoparticles, measuring C-terminal telopeptide of type I collagen (ICTP) concentration in supernatants, after 4 wk of immersion in artificial saliva. Numerical data were analyzed by analysis of variance (ANOVA) and Student-Newman-Keuls multiple comparisons tests ($p < .05$). Nanoparticles were effectively zinc-loaded and were shown to have a chelating effect, retaining calcium regardless of zinc incorporation. Nanoparticles failed to infiltrate demineralized intertubular dentin and remained on top of the hybrid layer, without altering bond strength. Calcium and phosphorus were found covering nanoparticles at the hybrid layer, after 24 h. Nanoparticle application in etched dentin also reduced MMP-mediated collagen degradation. Tested nanoparticles may be incorporated into dental adhesive systems to provide the appropriate environment in which dentin MMP collagen degradation is inhibited and mineral growth can occur.

KEY WORDS: remineralization, zinc, nanopolymers, hybrid layer, adhesives, dental.

DOI: 10.1177/0022034514551608

Received April 22, 2014; Last revision July 23, 2014; Accepted August 22, 2014

INTRODUCTION

The ultimate goal in the design of dental adhesives is to render durable adhesion to dentin and to protect the seed crystallite-sparse collagen fibrils of the scaffold from degradation. Re-incorporation of mineral into the demineralized dentin matrix is important since the mineral precipitated may work as a site for further nucleation, and the remineralized tissue may be more resistant to degradation (Liu *et al.*, 2011a).

To favor ion exchange and mineral precipitation within the hybrid layer, different particles have been incorporated into dental adhesives: bioactive glass, Portland cement, or amorphous calcium phosphate (Osorio *et al.*, 2012; Profeta, 2014). However, as minerals elute from the resins, there is a rapid decrease in their mechanical properties and bond strength over time (Sauro *et al.*, 2013a,b). Ceramic bioactive nanospheres, such as hydroxyaptite (HAp), have also been proposed as resin fillers (Besinis *et al.*, 2014), but they do not possess a controllable release and optimal degradation kinetics (Wu *et al.*, 2011). It has been reported that zinc acts as a matrix metalloproteinase (MMP) inhibitor (Osorio *et al.*, 2011) and stimulates hard-tissue mineralization (Hoppe *et al.*, 2011; Lynch *et al.*, 2011).

An alternative strategy in biomaterials is the use of polymeric particles as calcium- and phosphate-sequestering materials (*i.e.*, carboxylate-functionalized polymer particles that bind calcium). These polymers may also act as carriers of other biological factors for the management of tissue mineralization, permitting a controlled ion release rate (Leonor *et al.*, 2009; Wu *et al.*, 2011; Musyanovych and Landfester, 2014).

The aim of the present study was to incorporate zinc-loaded polymeric nanocarriers into a dental adhesive system without affecting bond strength, to determine if zinc could be released inhibiting MMP-mediated collagen degradation, favoring ion exchange for mineral precipitation at the hybrid layer.

The null hypotheses to be tested were that: (1) polymeric spheres are not bioactive (capable of forming a calcium-phosphate-rich layer, after simulated body fluid solution immersion) regardless of zinc loading; (2) nanosphere incorporation into a dental adhesive system does not affect dentin bond strength; and (3) zinc-loaded nanocarriers incorporated into adhesives do not inhibit MMP-mediated dentin collagen degradation.

MATERIALS & METHODS

PolymP-***n***Active nanoparticles (NPs) were purchased from NanoMyP (Granada, Spain). Particles were fabricated through polymerization precipitation. NPs are composed of 2-hydroxyethyl methacrylate as a backbone monomer, ethylene glycol dimethacrylate as a cross-linker, and methacrylic acid as a functional monomer.

Zinc-loading and Bioactivity Test

Since surface mineralization is difficult to investigate at nanometer detail, microparticles with identical composition (PolymP-*μ*Active from nanoMyP) were included in only this part of the study. For zinc-loading, 100 mg of particles were incubated at room temperature for 3 hr under gentle stirring in 20 mL of a solution of $ZnCl_2$ 0.1 (w/w%) (pH 7.5), centrifuged, washed with 20 mL of distilled water, and dried in a vacuum oven at 40°C to constant weight.

Micro- and nanospheres with and without zinc-loading were soaked in 20 mL of a simulated body fluid solution (SBFS) (reagents *per* 1,000 mL of SBFS: 8.035 g of NaCl, 0.355 g of $NaHCO_3$, 0.225 g of KCl, 0.231 g of $K_2HPO_4 \cdot 3H_2O$, 0.311 g of $MgCl_2 \cdot 6H_2O$, 39 g of 1M HCl, 0.292 g of $CaCl_2$, 0.072 g of Na_2SO_4, 118 g of Tris, 0 to 5 mL of 1M HCl for final pH adjustment) (pH 7.45) in sterile flasks for 7 days (Leonor *et al.*, 2009). After being dried, surfaces of polymeric spheres were analyzed by high-resolution scanning electron microscopy (SEM) (GEMINI, Carl Zeiss SMT, Jena, Germany) at 3 Kv and 4- to 5-mm working distance. Nanospheres were further examined by transmission electron microscopy (TEM) (LIBRA 120 PLUS, Carl Zeiss SMT). Both microscopes were attached to energy-dispersive analysis systems (EDX) (Inca 300 and 350, Oxford Instruments, Oxford, UK). To probe for amorphous mineral depositions, we performed x-ray diffraction analysis on NPs (Bruker D8 Advance; XRD Bruker Corporation, Vienna, Austria); conditions were CuKα radiation in θ−θ scan, in a range 2 Theta from 0° to 60°. All tests were performed in triplicate.

ICTP Determinations

Thirty sound unerupted human third molars were extracted with written informed consent from donors, under a protocol approved by the Institutional Review Board. Four dentin beams (0.75 mm x 0.75 mm x 5.0 mm) were obtained *per* molar, as described in Osorio *et al.* (2012). Specimens were demineralized by 10% phosphoric acid (pH 1.0) (Panreac Química, Barcelona, Spain) for 12 hr at 25°C. Demineralized dentin beams were rinsed in deionized water under constant stirring at 4°C for 72 hr. Dentin beams were distributed among the following groups: (1) no resin infiltration, or infiltrated with (2) Single Bond (3M ESPE, St. Paul, MN, USA) (SB), (3) nanoparticle (NPs) infiltration followed by SB, or (4) zinc-loaded nanoparticle (Zn-NPs) infiltration followed by SB. For NP infiltration, dentin beams were immersed in an ethanol suspension containing the NPs (density: 32 mg/mL) for 30 s. For resin infiltration, beams were immersed in the different resin mixtures for 12 hr under agitation. The demineralization and resin immersion processes were performed at 25ºC, in the dark. The samples were irradiated in different positions for 40 s until the entire area was exposed. The lamp was tested for light output (600 mW/cm^2). Two dentin beams from the same group were placed in Eppendorf tubes containing artificial saliva. Dentin specimens were incubated in 500 μL of artificial saliva at 37ºC. After 4 wk, sample volumes of 100 μL of the solution were withdrawn and analyzed for the liberation of collagen degradation product (C-terminal telopeptide of type I collagen [ICTP]) by means of a radioimmunoassay kit (ICTP-RIA Cat. No. 68601, Orion Diagnostica Oy, FI-02101 Espoo, Finland) (Osorio *et al.*, 2012).

Microtensile Bond Strength

Fifteen human third molars were horizontally sectioned below the dentin-enamel junction and ground flat (180-grit). Dentin surfaces were treated following manufacturer's instructions (phosphoric-acid-etching, washing, and drying). Before SB resin was applied, an ethanol suspension of NPs, Zn-NPs, or just ethanol was applied (30 s), respectively, in each of the 3 different experimental groups. Ethanol was gently evaporated for 30 s, and SB resin was finally applied. A composite build-up was performed (Tetric EvoCeram, Ivoclar-Vivadent, Schaan, Liechtenstein). Resin-bonded specimens were stored in deionized water at 37ºC for 24 hr. Bonded teeth were sectioned into 10 beams (area, 1 mm^2) and tested attached to a modified Bencor Multi-T testing apparatus (Danville Engineering Co., Danville, CA, USA) to failure in tension in a universal testing machine (Instron 4411; Instron Corporation, Canton, MA, USA) at a crosshead speed of 0.5 mm/min. Fractured specimens were examined with a stereomicroscope (Olympus SZ-CTV; Olympus, Tokyo, Japan) at 40x magnification to determine the mode of failure. Selected debonded sticks were observed by SEM, including EDX analysis.

Statistical Analysis

ICTP concentrations and microtensile bond strength (μTBS) values were analyzed by analysis of variance (ANOVA) and Student-Newman-Keuls multiple comparisons ($p < .05$).

RESULTS

Zinc Particle-loading and Bioactivity Test

SEM and TEM images are presented in Figs. 1 and 2. Microparticles were approximately 2.5 μm in diameter. NPs were 350 nm in diameter and did not agglomerate. Particles were spherical (Fig. 1). Some concentric, more dense subsurface structures were found on microparticles (Fig. 1b). On NPs, no traces of mineral elements were detected by EDX/SEM. Calcium was detected by EDX/SEM on microparticle surfaces after SBFS immersion, regardless of zinc loading (Figs. 1g, 1h). These deposits were evidenced as rounded agglomerates uniformly distributed on the microparticle surfaces. Microparticles lost their round shape after surface depositions occurred (Fig. 1g). No traces of zinc were evidenced by EDX/SEM. Elemental analysis on TEM was performed only for NPs and confirmed the effective zinc adsorption (Fig. 2b). Ca was identified in NPs that were zinc-loaded, before SBFS immersion (Fig. 2b). Calcium was also detected by EDX/TEM in NPs after SBFS immersion, regardless of zinc-loading (Figs. 2c, 2d). Nanocrystal formation was encountered in particles without zinc, after SBFS immersion (Fig. 2c). XRD patterns of NPs are presented in Fig. 3c. Amorphous composition is evidenced in all cases. Signs of initial crystal formation (low peaks at 11° and 32°) were seen only in spectra from Zn-NPs, after SBFS immersion.

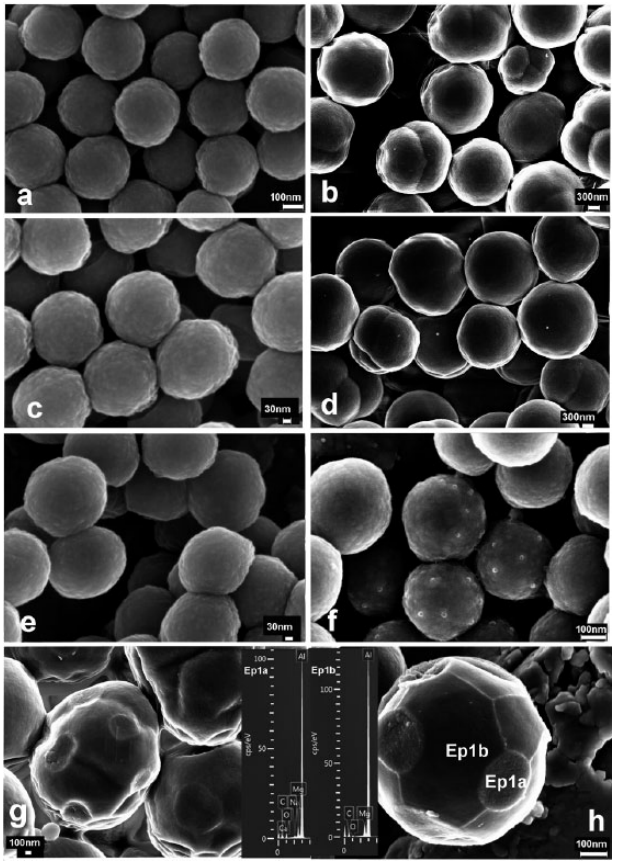

Figure 1. Scanning electron microscopy (SEM) micrographs of nanoparticles (NPs) and microparticles. **(a)** NPs before immersion in simulated body fluid solution (SBFS) were spherical, around 350 nm in diameter. NPs did not agglomerate. **(b)** Microparticles before immersion in SBFS were 2.5 μm in diameter. Some concentric, more dense subsurface structures were found. **(c)** NPs after immersion in 0.1 w/w% $ZnCl_2$ for 3 hr. **(d)** Microparticles after immersion in 0.1 w/w% $ZnCl_2$ for 3 hr. **(e)** NPs after immersion in SBFS for 7 days**. (f)** Zn-NPs after 7 days' immersion in SBFS. Spotty deposits were distributed throughout nanoparticle surfaces. **(g)** Microparticles after immersion in SBFS for 7 days. Microparticles showing a heterogeneous composition of central concentric electron reflections and outer increased density are presented. Regularly distributed rounded mineral agglomerates were encountered. **(h)** Zinc-loaded microparticles after immersion in SBFS for 7 days. Spotty calcium deposits were uniformly distributed throughout particle surfaces, and other formations were grown, forming polygonal lines. Particles lost their regular morphology. Calcium was identified when the spectrum in the energy-dispersive analysis (EDX) was taken from rounded mineral agglomerates (Ep1a), and calcium was not present in these areas (Ep1b). Al and Mg, at the EDX spectra, were contaminant elements from the sample-holder.

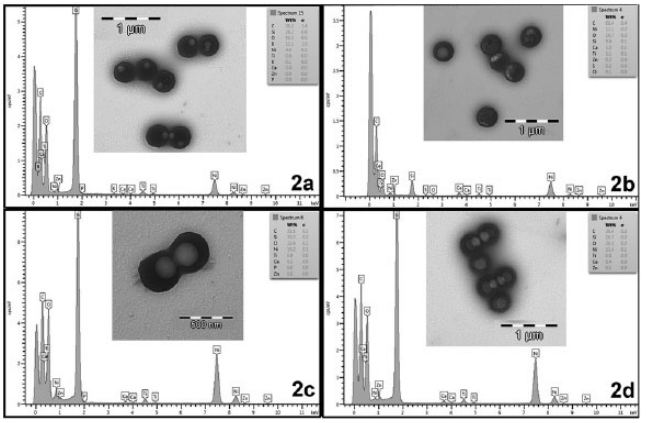

Figure 2. Transmission electron microscopic (TEM) images of nanoparticles (NPs). Light circular objects inside the NPs were artifacts that developed during electron beam transmission. Ni, Si, and Ti in the energy-dispersive analysis (EDX) spectra were contaminant elements from the sample holder. Scale bars are 1 micron and 500 nm in total length, as indicated. **(a)** NPs before Zn loading; zinc and calcium are absent in the EDX spectrum (Ep2a). **(b)** Zn-loaded NPs before immersion in simulated body fluid solution (SBFS). Zinc and calcium were detected in the EDX spectrum analysis (Ep2b). **(c)** NPs after immersion in SBFS for 7 days. Nanocrystals are observable on the particle surfaces. Calcium was identified (Ep2c). **(d)** Zn-NPs after 7 days in SBFS. Calcium and zinc were identified in the EDX spectrum (Ep2d).

Microtensile Bond Strength

Mean microtensile bond strength (μTBS) values and modes of failure are reported in the Table. μTBS values of tested resin were similar for all tested groups, with mean values ranging from 32 to 27 megaPascals (MPa). After SEM examination of debonded dentin surfaces (Figs. 3a, 3b), it was observed that NPs remained embedded on the hybrid layer and were homogeneously distributed on the dentin surface. NPs did not agglomerate and penetrated dentin tubules. NPs increased in size. Some polymeric NPs were found to be covered by calcium and phosphorus (Fig. 3; Ep3a), while others, rougher and bigger in size, also incorporated silicon (Fig. 3; Ep3b). Calcium was co-localized with the silica NPs in SB-bonded specimens (Fig. 3; Ep3c).

ICTP Determination

Mean ICTP concentration values were affected by different resin infiltration ($F = 323.45$; $p < .001$). Means and standard deviations of ICTP concentrations, liberated from the dentin beams, are listed in the Table. ICTP values at 4 wk followed the trend: no resin > neat resin > resin with NPs > resin with Zn-NPs.

DISCUSSION

The tested null hypotheses had to be partially rejected, since polymeric nanospheres were successfully loaded with zinc and were able to chelate calcium, regardless of zinc loading. NPs were not bioactive *in vitro* but were able to sequester calcium and phosphate in the presence of silicon, when effectively embedded at the hybrid layer. NP incorporation did not alter bond strength and inhibited MMP-mediated dentin collagen degradation.

Polymeric spheres were successfully loaded with zinc (Fig. 2b). Surfaces of these particles exhibited a high concentration of functional groups (COO^-) capable of complexing metal cations. Those particles immersed in $ZnCl_2$ solution not only acquired zinc but also retained calcium (Fig. 2b) because of the potent chelating effect exerted by these carboxyl-terminated polymers (Li *et al.*, 2013) and because of the presence of some calcium

impurities in the solution. Surface functional groups were also responsible for the presence of calcium in those particles, regardless of zinc loading. Ca precipitations were observed by SEM and TEM (Figs. 1g, 1h, 2c, 2d). Nanocrystal formations were encountered on non-zinc-loaded NP surfaces (Fig. 2c). It may be that the presence of zinc retarded calcium compound crystallization (Horiuchi *et al.*, 2009). An amorphous pattern of calcium deposits was observed at the XRD analysis. These amorphous compounds provide a local ion-rich environment that may be considered favorable for dentin remineralization (Gu *et al.*, 2011; Liu *et al*., 2011b). Characteristic peaks of scholzite [$CaZn_2$ $(PO_4)_2$. $2H_2O$] at 32° and 11° are observed in XRD spectra of Zn-NPs (Fig. 3c). This ion substitution may be explained on the basis of the difference in the ionic radii of calcium (0.099 nm) and zinc (0.074 nm). If the ionic radii are much smaller, it is easy to fill a vacancy or interstitial sites of crystal lattice (Song *et al.*, 2009; Osorio *et al.*, 2014). Phosphorus was not identified, so the calcium precipitations (Fig. 1h) and calcium crystal formations (Fig. 2c) probably correspond with calcium hydroxide and/or calcium carbonate compounds (HAp precursors) (Watson *et al.*, 2014). Crystal formations were not detected in XRD analysis because of their small size and proportion with respect to the amorphous phase. In XRD spectra, the ratio of peak intensities varies linearly as a function of weight fractions.

When NPs were applied to etched dentin, they remained embedded on the top of the hybrid layer (Figs. 3a, 3b), yet they did not alter the μTBS. Tested NPs had a diameter of 350 nm, higher than interfibrillar space widths, that prevented them from passing into hybrid layers (Besinis *et al.*, 2012). However, when particles smaller than 20 nm were applied, infiltrative capability deeper into the demineralized dentin was reduced because of particle agglomeration and/or particle binding to demineralized collagen (Besinis *et al.*, 2012). NP collagen binding is necessary to exert the remineralization effect. Inability of the NPs to bind to the collagen will lead to limited remineralization potential (Li *et al.*, 2013; Besinis *et al.*, 2014). Demineralization of dentin resulted in positively charged collagen (Besinis *et al.*, 2012), showing high affinity to the negatively charged (-43.3 mV) polymeric tested nanoparticles, finally leading to particle retention at the dentin surface. Particles were seen without agglomerate (due to their negative zeta potential) inside the dentinal tubules and on the hybrid layer (Figs. 3a, 3b).

Different NPs were encountered on the hybrid layer. Some NPs were covered by Ca and P, while others also contained silicon, and silica fillers from SB also contained calcium (Figs. 3a, 3b). The presence of silicon may be important, since silicon is known to facilitate CaP deposition on particles (Leonor *et al.*, 2009), and played a critical role in the binding of CaP to the collagen network (Besinis *et al.*, 2014). Silica NPs have been shown to mediate the formation of CaP precursors, necessary for the subsequent steps of mineralization, acting as a nucleating mineral (Watson *et al.*, 2014). Besinis *et al.* (2014) applied silica and HAp nanoparticles to demineralized dentin and hypothesized that phosphorus binds to silica NPs, thus enhancing remineralization when combined with ionic calcium. However, silica particles were covered by calcium (Fig. 3b; -Ep3c-), probably forming calcium silicate, which is a bioactive compound that can bind phosphorus (Profeta, 2014).

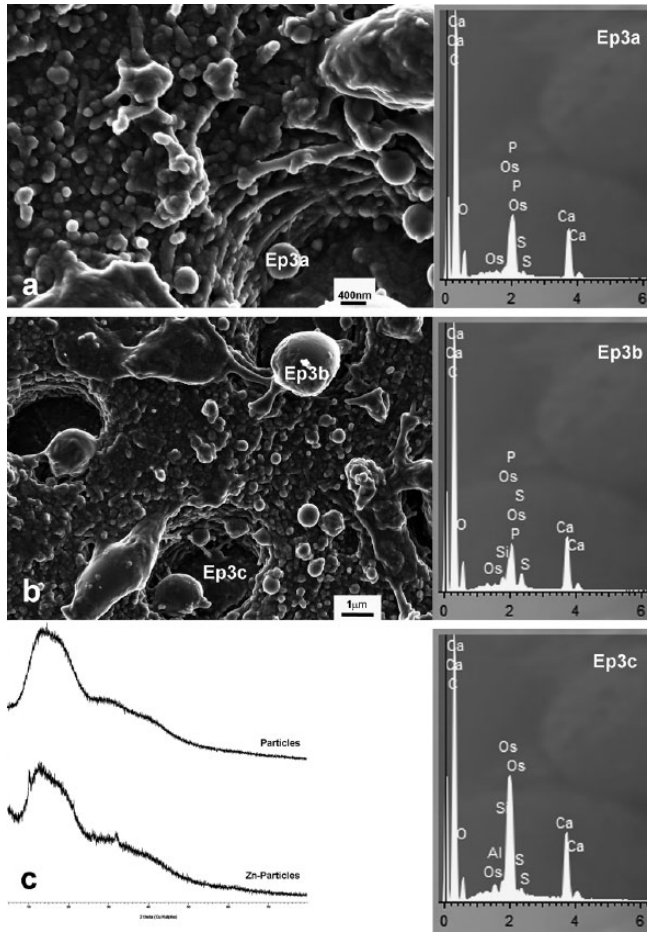

Figure 3. Scanning electron microscopy (SEM) micrographs of debonded dentin surfaces after microtensile bond strength (μTBS) and X-ray diffraction (XRD) spectra from nanoparticles. **(a, b)** Debonded dentin infiltrated with nanoparticles (NPs) and Single Bond (SB), after μTBS testing. NPs remained embedded in the hybrid layer and were homogeneously distributed on the dentin surface. NPs did not agglomerate, but seemed to penetrate dentin tubules. Some NPs were increased in size and measured up to 1 micron. Some of these NPs were found to be covered by calcium and phosphorus (Ep3a). Rougher NPs also incorporated silicon (Ep3b). Silica fillers from SB also contained calcium (Ep3c). (c) XRD spectra of particles after 7 days of simulated body fluid solution (SBFS) immersion with an amorphous pattern and Zn particles after 7 days of immersion, with 2 distinguished peaks at 11° and 32°, determining a compatible spectrum with initial scholzite crystal formation. Scholzite is $CaZn_2$ $(PO_4)_2.2H_2O$.

Considering the complexity of remineralization events and the many types of mineral formation that may take place, whether tested NPs are able to promote intrafibrillar mineral formation remains to be ascertained. It is unknown if the mineral is restricted to the surface or if ions may travel into the depth of dentin, and the coupling between the collagen fibrils and the CaP present at the NPs is not demonstrated. Research is needed to determine if these NPs may function as biomimetic analogs. Other polymers have been shown to mimic the

Table. Means and Standard Deviations of Telopeptide of Type I Collagen (ICTP) Concentration (μg/L) in Artificial Saliva after 4 wk of Immersion and Microtensile Bond Strength (in megaPascals, MPa) to Dentin and Mode of Failure of Experimental Groups

			Mode of Failure (%)		
	ICTP (μg/L) (n = 15)	μTBS MPa (n = 50)	A	C	M
Demineralized dentin	220.13 (15.32) A	XX	X	X	X
Resin	14.40 (2.12) B	32.44 (6.31) a	0	0	100
Resin with NPs	5.6 (1.02) C	28.45 (7.22) a	10	0	90
Resin with Zinc-NPs	0.1 (0.02) D	27.06 (6.77) a	5	0	95

Abbreviations: μTBS, microtensile bond strength to dentin; NPs, nanoparticles; Zinc-NPs, zinc-loaded nanoparticles; A, adhesive; C, cohesive; M, mixed. For each vertical column, values with identical letters indicate no statistically significant difference by Student-Newman-Keuls test ($p > .05$).

functions of dentin proteins (Li *et al.*, 2013). Biomimetic systems, *i.e.*, the combination of polycarboxylic acids (such as polyacrylic or polymethacrylic acids), have resulted in ordered intrafibrillar nanoapatite assembly (Gu *et al.*, 2011; Liu *et al.*, 2011b).

MMP activity was reduced after resin infiltration of completely demineralized dentin (Osorio *et al.*, 2012). Control demineralized dentin released 220 μg/L of ICTP. Resin-infiltrated beams liberated 14.4 μg/L ICTP. The large reduction in ICTP release may have been due to resins physically enveloping the matrix to prevent outward diffusion of any ICTP telopeptide fragments. Alternatively, the resins may have infiltrated the active sites of matrix MMPs, thereby inactivating them. Demineralized beams coated with NP and then resin-infiltrated released significantly less ICTP than did beams treated only with resin. Demineralized beams treated with Zn-doped NPs, and then resin-infiltrated, released even less ICTP than beams treated with NP without Zn and resin-infiltrated. Zinc has been shown to exert collagen protection from MMP degradation (Osorio *et al.*, 2011) and to induce dentin remineralization at the bonded interface (Toledano *et al.*, 2012, 2013). The effect of NP or Zn-doped NP treatment without resin infiltration was not tested. Future experiments should determine the effects of NanoMyP filler particles alone, without resin infiltration, on ICTP liberation. Skarja *et al*. (2009) reported that hydroxamic-containing polymers lowered the enzyme activity of activated MMPs. A physical interaction and binding mechanism between the active-site zinc of MMPs and the hydroxamic acid functional groups (COO^-) at NP surfaces was demonstrated. Tested NPs would produce a similar inhibitory effect. However, some dentinal MMPs were inaccessible to the COO^- groups, because NPs could not penetrate the interfibrillar spaces. Therefore, the 62% drop in ICTP release (when non-Zn-loading NPs were used) may also be accounted for by other factors and not attributed only to the COO^- groups' MMP binding ability.

Future research should be done on the activity of NPs to release various ions in a sustained manner and to determine how high zinc ion concentrations can be without causing cellular toxicity. NPs can also be conjugated with various therapeutic molecules. A polymeric sphere system able to combine bioactivity with a capacity for controlled protein/drug-delivery is ideal not only for teeth but also for bone regeneration (Wu *et al.*, 2011).

This investigation confirms the ability of zinc-nanoparticles to bind to demineralized dentin and remain on the hybrid layer, after resin infiltration. Resin infiltration greatly reduced the rate of ICTP liberation from dentin matrices, which reach the lowest values when Zn-NPs are present. Polymer nanoparticles may be useful in dentin bonding, when etch-and-rinse adhesives are used.

ACKNOWLEDGMENTS

This work was supported by grants MINECO/FEDER MAT2011-24551 and CEI-Biotic from UGR. The authors declare no potential conflicts of interest with respect to the authorship and/or publication of this article.

REFERENCES

Besinis A, van Noort R, Martin N (2012). Infiltration of demineralized dentin with silica and hydroxyapatite nanoparticles. *Dent Mater* 28:1012-1023.

Besinis A, van Noort R, Martin N (2014). Remineralization potential of fully demineralized dentin infiltrated with silica and hydroxyapatite nanoparticles. *Dent Mater* 30:249-262.

Gu LS, Kim YK, Liu Y, Takahashi K, Arun S, Wimmer CE, *et al*. (2011). Immobilization of a phosphonated analog of matrix phosphoproteins within cross-linked collagen as a templating mechanism for biomimetic mineralization. *Acta Biomater* 7:268-277.

Hoppe A, Güldal NS, Boccaccini AR (2011). A review of the biological response to ionic dissolution products from bioactive glasses and glass-ceramics. *Biomaterials* 32:2757-2774.

Horiuchi S, Asaoka K, Tanaka E (2009). Development of a novel cement by conversion of hopeite in set zinc phosphate cement into biocompatible apatite. *Biomed Mater Eng* 19:121-131.

Leonor IB, Balas F, Kawashita M, Reis RL, Kokubo T, Nakamura T (2009). Biomimetic apatite deposition on polymeric microspheres treated with a calcium silicate solution. *J Biomed Mater Res B Appl Biomater* 91:239-247.

Li J, Yang J, Li J, Chen L, Liang K, Wu W, *et al*. (2013). Bioinspired intrafibrillar mineralization of human dentine by PAMAM dendrimer. *Biomaterials* 34:6738-6747.

Liu Y, Li N, Qi YP, Dai L, Bryan TE, Mao J, *et al*. (2011a). Intrafibrillar collagen mineralization produced by biomimetic hierarchical nanoapatite assembly. *Adv Mater* 23:975-980.

Liu Y, Tjäderhane L, Breschi L, Mazzoni A, Li N, Mao J, *et al*. (2011b). Limitations in bonding to dentin and experimental strategies to prevent bond degradation. *J Dent Res* 90:953-968.

Lynch RJ, Churchley D, Butler A, Kearns S, Thomas GV, Badrock TC, *et al*. (2011). Effects of zinc and fluoride on the remineralisation of artificial

carious lesions under simulated plaque fluid conditions. *Caries Res* 45:313-322.

Musyanovych A, Landfester K (2014). Polymer micro- and nanocapsules as biological carriers with multifunctional properties. *Macromol Biosci* 14:458-477.

Osorio R, Yamauti M, Osorio E, Ruiz-Requena ME, Pashley DH, Tay FR, *et al*. (2011). Zinc reduces collagen degradation in demineralized human dentin explants. *J Dent* 39:148-153.

Osorio R, Yamauti M, Sauro S, Watson TF, Toledano M (2012). Experimental resin cements containing bioactive fillers reduced MMPs mediated dentin collagen degradation. *J Endod* 38:1227-1232.

Osorio R, Osorio E, Cabello I, Toledano M (2014). Zinc induces apatite and Scholzite formation during dentin remineralization. *Caries Res* 48:276-290.

Profeta AC (2014). Dentine bonding agents comprising calcium-silicates to support proactive dental care: origins, development and future. *Dent Mater J* 33:443-452.

Sauro S, Osorio R, Fulgencio R, Watson TF, Cama G, Thompson I, *et al*. (2013a). Remineralisation properties of innovative light-curable resin-based dental materials containing bioactive micro-fillers. *J Mater Chem B* 1:2624-2638.

Sauro S, Osorio R, Osorio E, Watson TF, Toledano M (2013b). Novel light-curable materials containing experimental bioactive micro-fillers remineralise mineral-depleted bonded-dentine interfaces. *J Biomater Sci Polym Ed* 24:940-956.

Skarja GA, Brown AL, Ho RK, May MH, Sefton MV (2009). The effect of a hydroxamic acid-containing polymer on active matrix metalloproteinases. *Biomaterials* 30:1890-1897.

Song W, Tian M, Chen F, Tian Y, Wan C, Yu X (2009). The study on the degradation and mineralization mechanism of ion-doped calcium polyphosphate in vitro. *J Biomed Mater Res B Appl Biomater* 89:430-438.

Toledano M, Yamauti M, Ruiz-Requena ME, Osorio R (2012). A ZnO-doped adhesive reduced collagen degradation favouring dentine remineralization. *J Dent* 40:756-765.

Toledano M, Sauro S, Cabello I, Watson T, Osorio R (2013). A Zn-doped etch-and-rinse adhesive may improve the mechanical properties and the integrity at the bonded-dentin interface. *Dent Mater* 29:e142-e152.

Watson TF, Atmeh AR, Sajini S, Cook RJ, Festy F (2014). Present and future of glass-ionomers and calcium-silicate cements as bioactive materials in dentistry: biophotonics-based interfacial analyses in health and disease. *Dent Mater* 30:50-61.

Wu C, Zhang Y, Fan W, Ke X, Hu X, Zhou Y, *et al*. (2011). $CaSiO_3$ microstructure modulating the in vitro and in vivo bioactivity of poly(lactide-co-glycolide) microspheres. *J Biomed Mater Res Part A* 98:122-131.